M&C 2017 - International Conference on Mathematics & Computational Methods Applied to Nuclear Science & Engineering,
Jeju, Korea, April 16-20, 2017, on USB (2017)

Criticality Benchmarks for the Finite-Element-with-Discontiguous-Support Multigroup Method

Pablo A. Vaquer & Ryan G. McClarren

Nuclear Engineering Department, Texas A&M University
mdcpablo@tamu.edu, rgm@tamu.edu

Abstract - *This study compared the efficiency of the multigroup method to the finite-element-with-discontiguous-support multigroup method (FEDS) for discretizing the energy domain for radiation transport simulations. FEDS is similar to multigroup in that the energy domain is first partitioned into coarse groups, but is different than multigroup in that it further partitions the coarse groups into discontiguous energy elements within each coarse group. This paper presents a procedure for propagating uncertainties for FEDS, followed by two verification problems to test if the uncertainty propagation routines were implemented correctly. The absolute error in the verification problems were* 6×10^{-8} *and* 5×10^{-8}*, respectively. Next the paper uses two criticality benchmarks which demonstrate that FEDS converges faster than multigroup to an energy-resolved solution. The absolute error in the two validations problems were* 2×10^{-4}*, and* 4×10^{-3}*, respectively.*

I. INTRODUCTION

Radiation-transport deterministic methods demand plenty of computer memory in order to discretize the space, angle, energy, and time domains. The energy domain, by itself, is difficult to discretize efficiently and accurately because nuclear cross sections can vary by several orders of magnitude due a small difference in an incident particle's energy, as shown in Fig.(1). In this study we compare different methods for discretizing the energy domain.

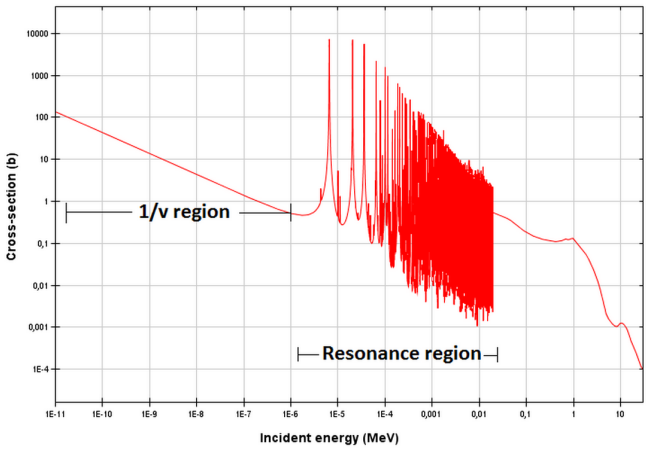

Fig. 1. Total microscopic cross section for ^{238}U.

The multigroup method is a deterministic method that discretizes energy into several contiguous intervals called groups. In the multigroup method, particles that have similar energies fall into the same energy group, and are treated the same as other particles within that energy group. The disadvantage of using the multigroup method is that thousands of energy groups are required to properly discretize the resolved-resonance region (RRR), unless a very accurate weighting flux is used generate the multigroup cross sections.

The finite-element-with-discontiguous-support multigroup method (FEDS) is a generalization of the Mutligroup method [1]. FEDS first decomposes the energy domain into coarse groups and then further partitions the coarse groups into discontiguous energy elements within each coarse group. A minimization problem is then solved in order to optimally cluster portions of the energy domain into discontiguous elements.

In this study, we used NJOY 2012 and a set of Python scripts to generate multigroup, FEDS, and continuous-energy cross sections. These scripts were also used to generate covariance matrices which were utilized to propagate uncertainties from a nuclear database to a quantity of interest. Two verification benchmarks were used to test if our uncertainty propagation scripts would produce the correct value for the variance in a quantity of interest. We then compared the convergence rates between multigroup and FEDS for two criticality benchmarks.

II. THEORY

1. Multigroup

The multigroup method partitions the energy domain into several contiguous energy groups. Group cross sections Σ_g are then computed such that reaction rates are conserved within each group,

$$\Sigma_g \psi_g = \int_{E_{g-1}}^{E_g} dE\, \Sigma(E)\psi(E)\,,$$

where $\psi(E)$ is the angular flux. However, $\psi(E)$ is not known before conducting the radiation transport simulation therefore we approximate $\psi(E)$ using a weighting function $w(E)$ which mimics the expected neutron spectrum and compute group cross sections as

$$\Sigma_g = \frac{\int_{E_{g-1}}^{E_g} dE\, w(E)\Sigma(E)}{\int_{E_{g-1}}^{E_g} dE\, w(E)}\,.$$

These group cross sections are then used in the steady-

state multigroup equation,

$$\left[\hat{\Omega}\cdot\nabla+\Sigma_{t,g}(\boldsymbol{r})\right]\psi_g(\boldsymbol{r},\hat{\Omega}) = \sum_{\ell=0}^{L}\sum_{m=-\ell}^{\ell}\frac{2\ell+1}{4\pi}Y_\ell^m(\hat{\Omega})\sum_{g'=1}\Sigma_{s,\ell,g'\to g}(\boldsymbol{r})\phi_{\ell,g'}^m(\boldsymbol{r})+ \frac{\chi_g(\boldsymbol{r})}{4\pi k}\sum_{g'=1}\nu\Sigma_{f,g'}(\boldsymbol{r})\Phi_{g'}(\boldsymbol{r})\,, \quad (1)$$

where

$\boldsymbol{r}$	position of particles in space
$\hat{\Omega}$	particles' direction of travel
$\phi_g(\boldsymbol{r})$	scalar flux for group g
$\psi_g(\boldsymbol{r},\hat{\Omega})$	angular flux for group g
$\Sigma_{t,g}(\boldsymbol{r})$	total macroscopic cross section for group g
$\Sigma_{s,\ell,g'\to g}(\boldsymbol{r})$	double-differential scattering cross section
$\chi_g(\boldsymbol{r})$	fission energy spectrum for group g
$\nu_{g'}(\boldsymbol{r})$	number of neutrons produced per fission
$\Sigma_{f,g'}(\boldsymbol{r})$	fission cross section for group g' .

Here $w(E)$ is assumed to have the same distribution in energy as the angular flux $\psi(E)$. The problem with this weighting technique is the angular flux may vary widely in different regions of the problem and also as a function of angle, and is unknown prior to the simulation, thus the weighting function $w(E)$ may not be similar enough to $\psi(\boldsymbol{r},\hat{\Omega},E)$ in order to properly conserve reaction rates. In addition, nuclear resonances in different materials don't necessarily fall within the same energy intervals, therefore a group structure that works well for one material doesn't necessarily work well for all materials. Sometimes, the only way to conduct an accurate radiation transport simulation is to use very fine groups, but this is may not be feasible if a simulation also requires fine space, angle, and time discretizations.

2. FEDS

Unlike multigroup, FEDS only uses a few coarse groups, and these coarse groups are further partitioned into discontiguous energy elements within each coarse group [1]. For example, particles of energy 1 eV and 3 eV can reside within one energy element, and particles of energy 2 eV and 4 eV can reside within a different energy element. The idea behind FEDS is to minimize how much the particle flux varies within a single element. This is not a simple minimization problem, because the particle flux can vary drastically, even within the same material in a problem. For example, the neutron energy spectrum in the center of a fuel rod in a reactor is not the same as the neutron spectrum at the edge of the fuel rod. Thus, we first select a set of spectra that we want our finite element space to accurately represent. Next, we solve the following minimization problem to construct an optimized energy element mesh:

1. Given a set of spectra and energy subelements, arbitrarily map subelements into elements (the subelements are all small contiguous energy intervals and the elements can be composed of a discontiguous set of subelements).
2. Compute the averages of the spectra in each element.
3. Compute the difference between the continuous-energy spectrum and the element-averaged spectrum, and sum these differences over all elements and spectra. We will refer to this total difference as the *variance error*.
4. Choose the energy element mesh which minimizes the variance error by looking at all possible combinations of subelements into elements.

This variance error essentially measures the accuracy of resonance-scale behavior that is captured using a particular energy element mesh. There are several machine-learning algorithms for clustering subelements into elements, and iterating over possible combinations of subelements into elements to generate an optimal FEDS energy grid. These algorithms are discussed in detail by Till in [1].

A generalized Petrov-Galerkin finite element method can be defined for these discontiguous energy elements as

$$\varphi(\boldsymbol{r},\hat{\Omega},E)\equiv\sum_{e=1}^{N_e}\Psi_e(\boldsymbol{r},\hat{\Omega})b_e(\boldsymbol{r},E) \quad (2)$$

where

$$b_e(\boldsymbol{r},E)=\begin{cases}\frac{f_e(E)}{\int_{\mathbb{E}_e}dE\,f_e(E)} & \text{if } E\in\mathbb{E}_e,\\ 0 & \text{otherwise,}\end{cases} \quad (3)$$

and

$$w_e(E)=\begin{cases}1 & \text{if } E\in\mathbb{E}_e,\\ 0 & \text{otherwise .}\end{cases} \quad (4)$$

Here

$\varphi(\boldsymbol{r},\hat{\Omega},E)$	finite element angular flux
$\Psi_e(\boldsymbol{r},\hat{\Omega})$	angular flux for energy element e
$b_e(\boldsymbol{r},E)$	basis function
$\mathbb{E}_e$	energy element space for element e
$f_e(E)$	arbitrary weighting flux for element e
$w_e(E)$	weighting function for element e .

By substituting this basis-function representation of the angular flux into the transport equation, one can derive the steady-state FEDS transport equation,

$$\left[\hat{\Omega}\cdot\nabla+\Sigma_{t,e}(\boldsymbol{r})\right]\Psi_e(\boldsymbol{r},\hat{\Omega}) = \sum_{\ell=0}^{L}\sum_{m=-\ell}^{\ell}\frac{2\ell+1}{4\pi}Y_\ell^m(\hat{\Omega})\sum_{e'=1}\Sigma_{s,\ell,e'\to e}(\boldsymbol{r})\Phi_{\ell,e'}^m(\boldsymbol{r})+ \frac{\chi_e(\boldsymbol{r})}{4\pi k}\sum_{e'=1}\nu\Sigma_{f,e'}(\boldsymbol{r})\Phi_{e'}(\boldsymbol{r}) \quad (5)$$

Notice how the FEDS transport equation is very similar to the multigroup equation, Eq.(1), with the exception that the energy elements, e, are computed as weighted averages over the discontiguous support of the energy elements. The advantage

in solving the FEDS transport equation over the multigroup equation is that the FEDS elements are better at capturing resonance-scale behavior. However, the FEDS transport equation is more computationally expensive because the scattering matrix can be more dense in the resolved-resonance region (RRR) (namely, there can be lots of up- and down-scattering between different elements in the RRR).

3. Bondarenko Method

In order to generate FEDS or multigroup microscopic cross sections, the spectrum of particle energies must be known first, and spectra can vary widely for different geometries and materials. In our best attempt to preserve reaction rates in all space and directions, we begin with the steady-state transport equation

$$\hat{\Omega} \cdot \nabla\psi + \Sigma_t(\boldsymbol{r}, E)\psi(\boldsymbol{r}, \hat{\Omega}, E) = s(\boldsymbol{r}, \hat{\Omega}, E) \tag{6}$$

and integrate over all $\boldsymbol{r}$ and $\hat{\Omega}$ to get

$$J^+(E) - J^-(E) + \Sigma_t(E)\phi(E) = s(E)\,, \tag{7}$$

where

$\phi(E)$	scalar flux
$J^-(E)$	outward particle current
$J^+(E)$	inward particle current .

In order to solve for the flux we can make the following substitutions

$$\Sigma_e(E) = \frac{J^+(E)}{\phi(E)} \quad \text{and} \quad S(E) = s(E) + J^-(E)$$

and show that

$$\phi(E) \approx \frac{S(E)}{\Sigma_e + \Sigma_t(E)} \tag{8}$$

where $S(E)$ is the modified source rate which includes the inward particle current, and Σ_e is the escape cross section which takes leakage into account. There are many ways to approximate an escape cross section. For simplicity, in this study we approximated the escape cross section as the inverse of the mean chord length of a material's geometry.

The simplified solution for the scalar flux shown in Eq.(8) can be used as a geometry-averaged weighting function in order to weight multigroup or FEDS cross sections,

$$w(E) \approx \frac{S(E)}{\Sigma_e + \Sigma_t(E)}\,. \tag{9}$$

However, at this point $\Sigma_t(E)$ is still unknown. Therefore we must iterate to obtain our values for $w(E)$ and $\Sigma_t(E)$. Cross-section-generation codes typically produce microscopic cross sections for each isotopes separately, thus we can make the following substitution

$$\sigma_{0,i}(E) = \frac{1}{N_i}\Big(\Sigma_e + \sum_{j\neq i} N_j \sigma^{k-1}_{t,j}(E)\Big)\,,$$

to rewrite Eq.(9) in terms of microscopic cross sections,

$$w_i(E) \approx \frac{S(E)}{N_i\Big(\sigma_{t,i}(E) + \sigma_{0,i}(E)\Big)}\,,$$

where $\sigma_{t,i}$ is the total microscopic cross section for isotope i and $\sigma_{0,i}$ is the background cross section for isotope i. The background cross section includes any particle loss that is not caused by isotope i.

Bondarenko iterations can be used to produce self-consistent FEDS or multigroup microscopic cross sections for each energy group and each isotope in a material. A Bondarenko iteration consists of the following steps:

1. Calculate the background cross section $\sigma^k_{0,g,i}$ for iteration k,
$$\sigma^k_{0,g,i} = \frac{1}{N_i}\Big(\Sigma_e + \sum_{j\neq i} N_j \sigma^{k-1}_{t,g,j}\Big)\,.$$
In the first iteration the value of $\sigma^k_{0,g,i}$ is guessed.
2. Compute the weighting spectrum, based on the new background cross section,
$$w^k_i(E) \approx \frac{S(E)}{N_i(\sigma^k_{t,g,i} + \sigma^k_{0,g,i})}\,.$$
3. Compute the total cross section $\sigma^k_{t,g,i}$ for isotope i using the new weighting spectrum,
$$\sigma^k_{t,g,i} = \frac{\int_{E_g}^{E_{g-1}} dE\, w^k_i(E)\sigma^k_{t,i}(E)}{\int_{E_g}^{E_{g-1}} dE\, w^k_i(E)}\,.$$
Do this for all isotopes and groups.
4. Check if the following convergence criterion is satisfied,
$$\left\| \frac{\sigma^k_{t,g,i} - \sigma^{k-1}_{t,g,i}}{\sigma^k_{t,g,i}} \right\|_{L^\infty} < \epsilon\,.$$
If the convergence criterion is not satisfied, return to step 1 using the updated values for $\sigma^{k-1}_{t,g,j}$.

For FEDS, replace group g with element e in the iteration scheme list above.

4. Uncertain Parameters in Neutron Transport

For this portion of the theory section, we will limit our discussion to propagating uncertainties for the steady-state form of the neutron transport equation. The steady-state neutron transport is

$$\begin{aligned}\hat{\Omega} \cdot \nabla\psi + \Sigma_t(\boldsymbol{r}, E)\psi(\boldsymbol{r}, \hat{\Omega}, E) = \\ \int_{4\pi} d\Omega' \int_0^\infty dE'\, \Sigma_s(\boldsymbol{r}, \hat{\Omega}' \cdot \hat{\Omega}, E' \to E)\psi(\boldsymbol{r}, \hat{\Omega}', E') + \\ \frac{1}{k_{\text{eff}}} \frac{1}{4\pi} \int_0^\infty dE'\, \Sigma_f(\boldsymbol{r}, E' \to E)\psi(\boldsymbol{r}, \hat{\Omega}', E')\end{aligned} \tag{10}$$

and

$$\psi(\boldsymbol{r}, \hat{\Omega}, E, t) = f(\boldsymbol{r}, \hat{\Omega}, E, t) \quad \text{for } r \in \partial V,\ \hat{\Omega} \cdot \hat{n} < 0\,.$$

where the macroscopic cross section Σ_x for reaction x is the sum of microscopic cross section $\sigma_{i,x}$ of the constituent isotopes, weighted by the number densities of those isotope N_i,

$$\Sigma_x = \sum_{i=1}^{I} N_i \sigma_{i,x}$$

In Eq.(10), the fission source term contains a double-differential fission cross section $\Sigma_f(\boldsymbol{r}, E' \to E)$ (which is similar to a double-differential scattering cross section, except multiple neutrons can be produced per fission). This fission source term is physically accurate because the number of neutrons produced per fission and the energy of those neutrons is dependent on the incident neutron energy. However, it's important to note that typically the following approximation is made for the fission source term

$$\int_0^\infty dE'\, \Sigma_f(\boldsymbol{r}, E' \to E)\psi(\boldsymbol{r}, \hat{\Omega}', E') \approx \chi(E) \int_0^\infty dE'\, \nu\Sigma_f(\boldsymbol{r}, E')\psi(\boldsymbol{r}, \hat{\Omega}', E')\,. \quad (11)$$

where $\chi(E)$ is a steady-state fission spectrum for prompt and delayed neutrons, and ν is the average number of neutrons produced (prompt and delayed) per fission. Together Eq.(10) and Eq.(11) contain several uncertain parameters:

N_i	number density of isotope i
$\sigma_{t,i}(\boldsymbol{r}, E)$	total microscopic cross section
$\sigma_{s,i}(\boldsymbol{r}, \hat{\Omega}' \cdot \hat{\Omega}, E' \to E)$	double-differential scattering
$\chi_i(E)$	fission neutron energy spectrum
$\nu_i(\boldsymbol{r}, E')$	neutrons produced per fission
$\sigma_{f,i}(\boldsymbol{r}, E')$	fission cross section
∂V	location of boundary or interface
$f(\boldsymbol{r}, \hat{\Omega}, E)$	boundary condition

In order to properly propagate uncertainties, we need more than just the standard deviation of the uncertainty of each uncertain parameter. We also need the covariance between all uncertain parameters. The covariances between different isotopes at different energies are computed based on experimental data. The covariance between two parameters p_i and p_j is defined as

$$\text{cov}(p_i, p_j) = \langle p_i p_j \rangle - \langle p_i \rangle \langle p_j \rangle\,, \quad (12)$$

where $\langle \cdot \rangle$ is used to represent expected value. The covariance between all uncertain parameters can be represented by a covariance matrix. However, constructing a covariance matrix for all uncertain parameters is computationally expensive, and may be unnecessary since many parameters are uncorrelated.

We can reduce the size of the covariance matrix by assuming there is no correlation between the cross sections of different materials. This results in each material having it's own separate covariance matrix. While this assumption is valid for most materials, it is not the case for all materials. Furthermore, we can greatly reduce the size of this covariance matrix by determining the covariance between scattering cross sections (instead of double-differential scattering cross sections) by using the property

$$\text{cov}(\sigma_{s,g}, \sigma_{s,g}) = \sum_{g'=1}^{G} \sum_{g''=1}^{G} \text{cov}(\sigma_{s,g\to g'}, \sigma_{s,g\to g''}) \quad (13)$$

and compute sensitivity of the quantity of interest Q to $\sigma_{s,\ell,g}$ using the following relation was derived by Bruss in [2],

$$\frac{\partial Q}{\partial \sigma_{s,\ell,g}} = \sum_{g'=1}^{G} \frac{\partial Q}{\partial \sigma_{s,\ell,g}} \frac{\sigma_{s,\ell,g\to g'}}{\sigma_{s,g}}\,. \quad (14)$$

5. Uncertainty Propagation for FEDS

In order to propagate uncertainties for FEDS, we will first define the variance in some quantity of interest Q as

$$\text{var}(Q) = \sum_{i=1}^{P} \sum_{j=1}^{P} \frac{\partial Q}{\partial p_i} \frac{\partial Q}{\partial p_j} \text{cov}(p_i, p_j) \quad (15)$$

where p is used to represent any parameter which may affect the quantity of interest, and P is the total number of relevant parameters. These parameters can be cross sections for different interactions, at different incident-particle energies, in different materials as well as many other uncertain parameters.

Note that the value of $\text{cov}(p_i, p_j)$ could have some uncertainty itself which isn't being considered in Eq.(15). Also, high-order sensitivities of the quantity of interest (such as $\partial^2 Q/\partial p_i^2$) are not included in Eq.(15) which may be important for some uncertainty calculations.

To derive a covariance matrix for FEDS cross sections let's first assume σ_i and σ_j are cross sections for energy elements i and j, respectively, and are composed of a discontiguous set of subelements such that

$$\sigma_i = \frac{1}{\Delta E_i} \sum_{m=1}^{M} \Delta E_{i,m} \sigma_{i,m}$$

$$\sigma_j = \frac{1}{\Delta E_j} \sum_{n=1}^{N} \Delta E_{j,n} \sigma_{j,n}$$

where $\sigma_{i,m}$ and $\sigma_{j,n}$ are subelement cross sections, $\Delta E_{i,m}$ and $\Delta E_{j,n}$ are subelement bin widths, ΔE_i and ΔE_j are the sum of constituent subelements bin widths for elements i and j, and M and N are the total number of subelements within elements i and j. Now we can use the covariance property,

$$\text{cov}(aX + bY, Z) = a\,\text{cov}(X, Z) + b\,\text{cov}(Y, Z)$$

where a and b are constants, and X, Y, and Z are variables, to show that covariance between two element cross sections is a weighted sum of the covariances of their subelements,

$$\text{cov}(\sigma_i, \sigma_j) = \sum_{m=1}^{M} \sum_{n=1}^{N} \left(\frac{\Delta E_{i,m}}{\Delta E_i}\right)\left(\frac{\Delta E_{j,n}}{\Delta E_j}\right) \text{cov}(\sigma_{i,m}, \sigma_{j,n})\,. \quad (16)$$

Together Eq.(15) and Eq.(16) can be combined to estimate that the variance in the quantity of interest for FEDS.

Figure 2 shows an example of an element correlation matrix and it's corresponding subelement correlation matrix. A correlation matrix is simply a covariance matrix that is normalized such that there are ones along the main diagonal of the matrix.

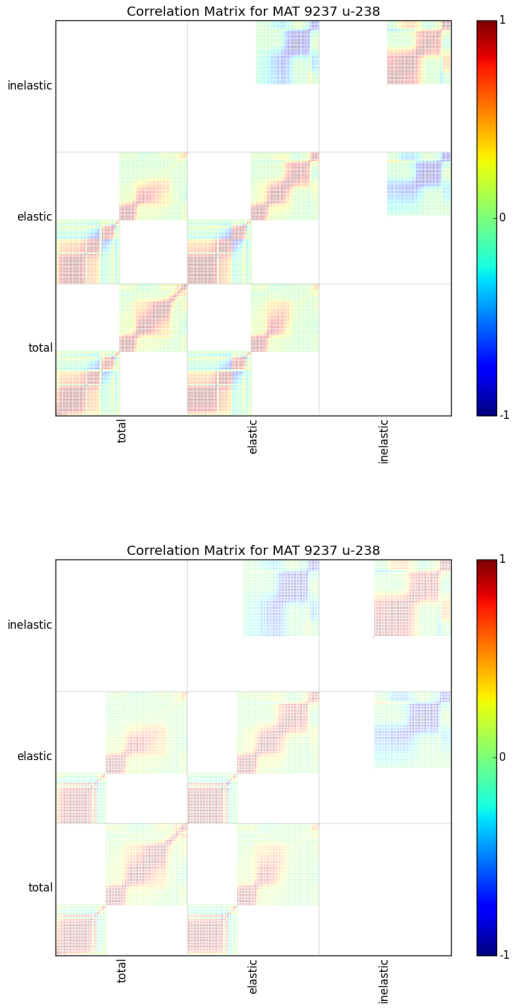

Fig. 2. Comparison of subelement correlation matrix (top) and an corresponding element correlation matrix (bottom) for ^{238}U generated using Barnfire for a coarse energy mesh.

III. RESULTS

Recently, a cross section generation framework known as Barnfire was developed at Texas A&M University. Barnfire leverages the Nuclear Data Processing System (NJOY) [3] and Parallel Deterministic Transport (PDT) [4] to generate cross sections and simulate radiation transport. Barnfire uses the Bondarenko method to construct accurate weighting spectra and it can generate multigroup, FEDS, and continuous-energy cross sections.

Two verification problems were used to determine if Barnfire was correctly propagating uncertainties and determine the correct variance in some quantity of interest. While, two validation criticality benchmarks were used to test Barnfire and compare the multigroup method to FEDS.

1. Verification Problem 1

The first verification problem is a pure-absorbing infinite-medium with an isotropic source of neutrons, where the quantity of interest Q is the reaction rate per unit volume, we can calculate Q by

$$Q = \langle \psi, q^\dagger \rangle$$

where $\langle \cdot, \cdot \rangle$ is an inner product over the relevant phase space,

$$\langle \cdot, \cdot \rangle \equiv \int_V dV \int_{4\pi} d\Omega \int_0^\infty dE$$

and

$$q^\dagger = \frac{\sigma_t}{V} .$$

The following arbitrary values for the source rate, cross sections, and the covariances were used for energy mesh which had 2 elements with each element was composed of 2 subelements of equal size,

$$\begin{pmatrix} s_1 \\ s_2 \end{pmatrix} = \begin{pmatrix} 2 \\ 2 \end{pmatrix}$$

$$\begin{pmatrix} \sigma_{t,1} \\ \sigma_{t,2} \end{pmatrix} = \begin{pmatrix} 1 \\ 2 \end{pmatrix}$$

$$\mathrm{cov}(\sigma_t, \sigma_t) = \begin{array}{c} \\ \sigma_{t,1,1} \\ \sigma_{t,2,1} \\ \sigma_{t,1,2} \\ \sigma_{t,2,2} \end{array} \begin{array}{c} \begin{array}{cccc} \sigma_{t,1,1} & \sigma_{t,2,1} & \sigma_{t,1,2} & \sigma_{t,2,2} \end{array} \\ \begin{pmatrix} 0.02 & 0.01 & 0 & 0 \\ 0.01 & 0.02 & 0.01 & 0 \\ 0 & 0.01 & 0.02 & 0.01 \\ 0 & 0 & 0.01 & 0.02 \end{pmatrix} \end{array}$$

$$\mathrm{cov}(\sigma_s, \sigma_s) = \begin{array}{c} \\ \sigma_{s,1,1} \\ \sigma_{s,2,1} \\ \sigma_{s,1,2} \\ \sigma_{s,2,2} \end{array} \begin{array}{c} \begin{array}{cccc} \sigma_{s,1,1} & \sigma_{s,2,1} & \sigma_{s,1,2} & \sigma_{s,2,2} \end{array} \\ \begin{pmatrix} 0.02 & 0.01 & 0 & 0 \\ 0.01 & 0.02 & 0.01 & 0 \\ 0 & 0.01 & 0.02 & 0.01 \\ 0 & 0 & 0.01 & 0.02 \end{pmatrix} \end{array}$$

The subscripts for the σ's in the covariance matrices represent the element and it's subelement, respectively. Also, we will assume the source rate has no uncertainty in this problem.

Now that we have prescribed all the values for the verification problem, we can derive the analytical solutions for Q and var(Q). For a 2-element pure-absorbing infinite medium, composed of only one isotope, the FEDS transport equation reduces to

$$\sigma_{t,1}\phi_1 = \sigma_{s,1\to1}\phi_1 + \sigma_{s,2\to1}\phi_2 + s_1$$

$$\sigma_{t,2}\phi_2 = \sigma_{s,1\to2}\phi_1 + \sigma_{s,2\to2}\phi_2 + s_2 .$$

where s is the source rate divided by the number density. The quantity of interest can now be expressed as

$$Q = \sum_{e=1}^{E} \int_{4\pi} d\hat{\Omega}\, \psi_e \sigma_{t,e} = \sigma_{t,1}\phi_1 + \sigma_{t,2}\phi_2 \,.$$

After deriving the appropriate expressions for the sensitivies of different parameters to the quantity of interest and plugging in the corresponding values for these expressions we get that

$$Q \;=\; s_1 + s_2 \;=\; 4$$
$$\mathrm{var}(Q) = 2.56 \,.$$

A simulation was then conducted in PDT using these predefines cross sections and covariances, and Barnfire was used to propagate uncertainties to provide an estimate of Q and var(Q) from the simulation. The results we obtained for Q and var(Q) listed in Table I.

TABLE I. Comparison of Analytical Results to Barnfire for Verification Problem 1

	Analytical	Barnfire	Absolute Error
Q	4.0	4.0	0
var(Q)	0.64	0.64	-6.13×10^{-8}

These results confirmed that the uncertainty propagation routines were implemented correctly and that Barnfire is capable of determining the variance of the reaction rate due to nuclear data uncertainty.

2. Verification Problem 2

The second verification problem is an isotropic-scattering infinite medium with a small fission source evenly-distributed in the medium. For simplification assume there are only 2 energy elements with 2 subelements of equal size in each element, where $\chi_1 = 1, \chi_2 = 0$, and

$$\begin{pmatrix} \sigma_{t,1} \\ \sigma_{t,2} \\ \nu\sigma_{f,1} \\ \nu\sigma_{f,2} \\ \sigma_{s,1\to1} \\ \sigma_{s,1\to2} \\ \sigma_{s,2\to1} \\ \sigma_{s,2\to2} \end{pmatrix} = \begin{pmatrix} 91 \\ 108 \\ 1 \\ 7 \\ 75 \\ 10 \\ 5 \\ 100 \end{pmatrix}$$

Now we'll prescribe some arbitrary values for the covariance matrix for a 2-element problem with 2 subelements within each element. We will assume that there are no cross-parameter covariances (note that this would not be true in a realistic problem because σ_t, $\nu\sigma_f$, and σ_s would in fact be correlated).

$$\mathrm{cov}(\sigma_t, \sigma_t) = \begin{array}{c} \\ \sigma_{t,1,1} \\ \sigma_{t,2,1} \\ \sigma_{t,1,2} \\ \sigma_{t,2,2} \end{array} \begin{array}{c} \begin{array}{cccc} \sigma_{t,1,1} & \sigma_{t,2,1} & \sigma_{t,1,2} & \sigma_{t,2,2} \end{array} \\ \begin{pmatrix} 1.0 & 0.2 & 0 & 0 \\ 0.2 & 1.0 & 0.2 & 0 \\ 0 & 0.2 & 1.0 & 0.2 \\ 0 & 0 & 0.2 & 1.0 \end{pmatrix} \end{array}$$

$$\mathrm{cov}(\nu\sigma_f, \nu\sigma_f) = \begin{array}{c} \\ \nu\sigma_{f,1,1} \\ \nu\sigma_{f,2,1} \\ \nu\sigma_{f,1,2} \\ \nu\sigma_{f,2,2} \end{array} \begin{array}{c} \begin{array}{cccc} \nu\sigma_{f,1,1} & \nu\sigma_{f,2,1} & \nu\sigma_{f,1,2} & \nu\sigma_{f,2,2} \end{array} \\ \begin{pmatrix} 1.0 & 0.2 & 0 & 0 \\ 0.2 & 1.0 & 0.2 & 0 \\ 0 & 0.2 & 1.0 & 0.2 \\ 0 & 0 & 0.2 & 1.0 \end{pmatrix} \end{array}$$

$$\mathrm{cov}(\sigma_s, \sigma_s) = \begin{array}{c} \\ \sigma_{s,1,1} \\ \sigma_{s,2,1} \\ \sigma_{s,1,2} \\ \sigma_{s,2,2} \end{array} \begin{array}{c} \begin{array}{cccc} \sigma_{s,1,1} & \sigma_{s,2,1} & \sigma_{s,1,2} & \sigma_{s,2,2} \end{array} \\ \begin{pmatrix} 1.0 & 0.2 & 0 & 0 \\ 0.2 & 1.0 & 0.2 & 0 \\ 0 & 0.2 & 1.0 & 0.2 \\ 0 & 0 & 0.2 & 1.0 \end{pmatrix} \end{array}$$

In addition, we will set the quantity of interest to be the reactivity of the system

$$Q \;=\; \rho \;=\; \frac{k-1}{k} \,.$$

Now that we have prescribed all the values for the verification problem, we can derive the analytical solutions for Q and var(Q). For a 2-element eigenvalue problem where $\chi_1 = 1$ and $\chi_2 = 0$, the transport equation simplifies to

$$\sigma_{t,1}\phi_1 = \sigma_{s,1\to1}\phi_1 + \sigma_{s,2\to1}\phi_2 + \frac{1}{k}\left(\nu\sigma_{f,1}\phi_1 + \nu\sigma_{f,2}\phi_2\right)$$
$$\sigma_{t,2}\phi_2 = \sigma_{s,1\to2}\phi_1 + \sigma_{s,2\to2}\phi_2 \,.$$

From here we can show that

$$\frac{\phi_2}{\phi_1} = \frac{\sigma_{s,1\to2}}{\sigma_{t,2} - \sigma_{s,2\to2}}$$

and

$$Q \;=\; \left(1 - \frac{1}{k}\right) \;=\; 1 - \frac{\sigma_{t,1} - \sigma_{s,1\to1} - \sigma_{s,2\to1}\left(\frac{\sigma_{s,1\to2}}{\sigma_{t,2}-\sigma_{s,2\to2}}\right)}{\nu\sigma_{f,1} + \nu\sigma_{f,2}\left(\frac{\sigma_{s,1\to2}}{\sigma_{t,2}-\sigma_{s,2\to2}}\right)} \,.$$

After deriving the appropriate expressions for the sensitivities of different parameters to the quantity of interest and plugging in the corresponding values for these expressions we get that the material is critical (reactivity is equal to zero),

$$Q = 0$$

and

$$\mathrm{var}(Q) = 0.4281 \,.$$

A simulation was then conducted in PDT using these predefines cross sections and covariances, and Barnfire was used to propagate uncertainties to provide an estimate of Q and var(Q) from the simulation. The results we obtained for Q and var(Q) listed in Table II.

These results confirmed that PDT and Barnfire's uncertainty propagation routines are capable of providing the variance in the reactivity for a criticality problem. Thus, we confident that the variance we obtain from PDT and Barnfire for experimental criticality benchmarks will be correct.

TABLE II. Comparison of Analytical Results to Barnfire for Verification Problem 2

	Analytical	Barnfire	Absolute Error
Q	0	-1.01×10^{-8}	-1.01×10^{-8}
var(Q)	0.10703	0.10703	-5.33×10^{-8}

3. Validation Problem 1

The first validation problem is an infinite medium of highly-enriched uranium (HEU), and the quantity of interest is the criticality factor, k_{eff}. Table III shows the concentration of uranium isotopes in the HEU.

TABLE III. Concentration of isotopes in HEU.

isotope	number density [$\frac{\text{atoms}}{\text{barn-cm}}$]
^{234}U	4.9184×10^{-4}
^{235}U	4.4994×10^{-2}
^{238}U	2.4984×10^{-3}

Barnfire was used to generate FEDS, multigroup, and continuous-energy cross sections for all three isotopes (with nuclear data from the ENDF/B-VII.1 cross section library). The multigroup method split up the RRR into logarithmically spaced energy groups. Meanwhile, FEDS decomposed the RRR into 25 logarithmically-spaced coarse groups with varying number of elements per coarse group, depending on the simulation. Figure 3 provides an example of how Barnfire decomposed the RRR for FEDS using 75 energy elements. These multigroup and FEDS energy grids were used in separate PDT simulations.

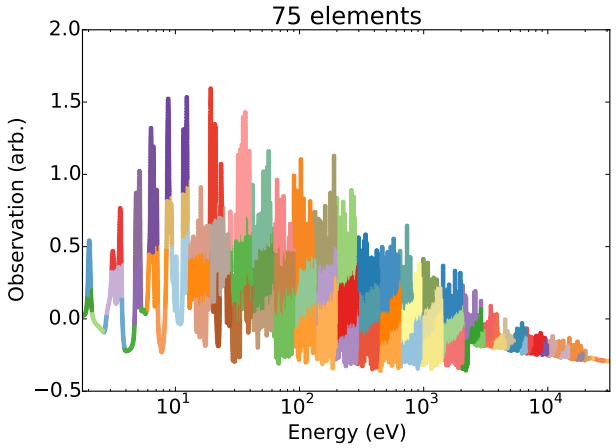

Fig. 3. This demonstrates how Barnfire partitions the resolved-resonance region of the energy domain into 25 logarithmically-spaced coarse-groups with 3 elements per coarse group, for a total of 75 elements.

The neutron spectrum generated by PDT using multigroup cross sections with 75 groups in the RRR was compared to the neutron spectrum generated by MCNP6 [5] using continuous-energy cross sections, as shown in Fig.(4). The neutron spectrum generated by PDT using FEDS cross sections with 75 elements in the RRR was also compared to the neutron spectrum generated by MCNP6 [5] using continuous-energy cross sections, as shown in Fig.(5). Notice how FEDS does a better job of capturing the resonance-scale behavior in comparison to multigroup.

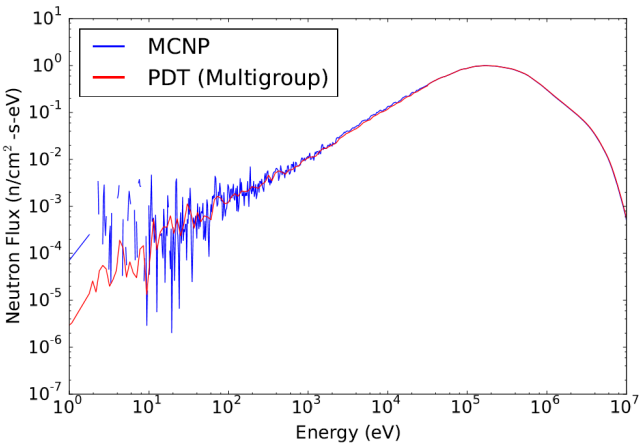

Fig. 4. Comparison of the multigroup neutron spectra in PDT to a continuous-energy neutron spectrum in MCNP6. This multigroup simulation used 75 groups in the RRR.

Afterwards, we compared the convergence rate of k_{eff} between using multigroup and FEDS in the RRR. Table IV shows the energy grid that was used for this particular study, and Figure 6 compares the convergence rates between FEDS and multigroup. Note in Table IV that only 14 groups are used in the thermal energy range. The reason for this is that HEU generates a fast neutron spectrum. Thus a small fraction of neutrons down-scatter all the way to the thermal energy range, so using 14 thermal groups is sufficient for this problem. Convergence studies were used to determine the number of groups that were needed in the unresolved-resonance range (URR). We determined that 250 were needed to reduce the absolute error in this high energy range to less than 10^{-5}. By ensuring that the thermal and URR energy grids are fully-resolved, we narrowed down our source of discretization error to only the energy resolution of the RRR.

As shown in Fig.(6) and Fig.(7), the multigroup and FEDS values for k_{eff} agree when there are 25 degrees of freedom in the RRR because in this case the FEDS simulation has 25 coarse groups with just a single element within each coarse group, so it is essentially just a multigroup method. Figure 7 demonstrates how FEDS converges much faster to within

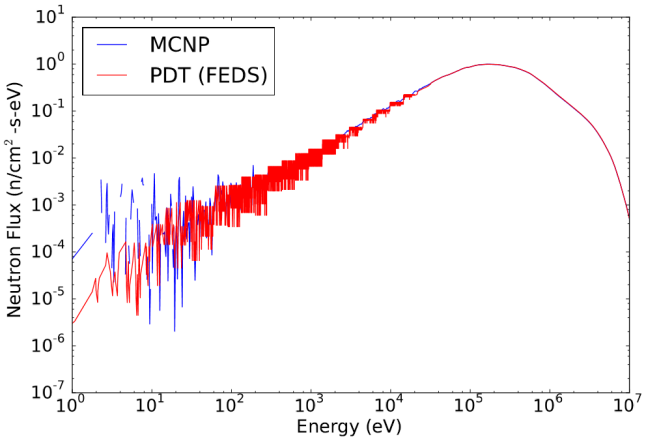

Fig. 5. Comparison of the FEDS neutron spectra in PDT to a continuous-energy neutron spectrum in MCNP6. This FEDS simulation used 75 elements in the RRR.

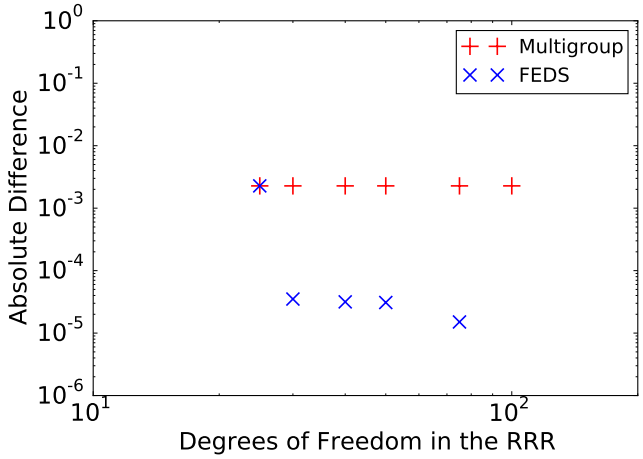

Fig. 6. This plot shows the discrepancy between the multigroup and FEDS values for k_{eff} from a reference solution which is fully-resolved in energy for validation problem 1 (the reference solution in this case is the FEDS value for k_{eff} with 100 elements in the RRR).

error margins of the continuous-energy value for k_{eff} than the multigroup method.

4. Validation Problem 2

The second validation problem is Godiva, a sphere of HEU with a radius of 8.7407 cm. This benchmark problem is the same as Validation Problem 1 except the geometry is spherical (refer to the description of Validation Problem 1 for material specifications). The criticality factor for Godiva was determined experimentally to be one. The difficulty of using PDT for this benchmark is that PDT currently only has two options for spatial discretization, a 3D Cartesian mesh and a triangular mesh in the X-Y plane which can be extruded along the Z axis to construct a 3D geometry. For this benchmark, PDT's triangular mesh was used to approximate the sphere of

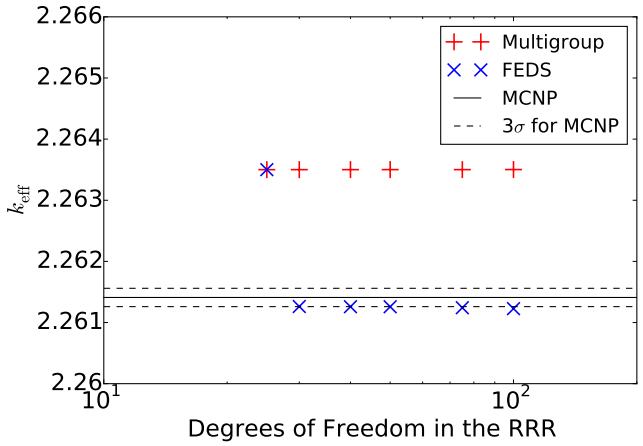

Fig. 7. This plot demonstrates how the FEDS value for k_{eff} quickly falls within the error bounds of MCNP6's continuous-energy solution while the multigroup solution is very slow to converge.

TABLE IV. Energy grid used for PDT simulations

Energy Range	Number of Elements
thermal (< 1.7eV)	14
RRR (1.7eV —31keV)	*variable*
URR (> 31keV)	250

HEU, as shown in Figure 8.

The same energy discretization for Validation Problem 1, shown in Table IV, was also used for Validation problem 2. In Validation Problem 2, we also used 16 quadrature angles per octant for the PDT discrete-ordinates calculation, and P_3 as the highest Legendre-moment for the scattering kernel. Due to computational resource constraints we did not run a Godiva simulation that was fully resolved in space, energy and angle. However, we were mostly interested in comparing the energy-discretization converge rates between FEDS and multigroup. The convergence rates of k_{eff} for Godiva are shown in Fig.(9). These results were very similar to the convergence rates for the infinite medium problem. However, Fig.(10) shows neither method approaches the experimental value of $k_{\text{eff}} \approx 1$. The results from Validation Problem 1 gives us confidence that most of the discrepancy in Validation Problem 2 is generated by spatial and angular discretization error, rather than cross section error.

IV. CONCLUSIONS

To summarize, FEDS is generalization of the multigroup method in which coarse groups can be further partitioned into discontiguous energy elements. The energy element mesh for FEDS is constructed such that the variation of the continuous-energy cross section within an element is minimized. This allows FEDS to capture resonance scale behavior more easily than multigroup. The two verification problems that were used provided confidence that Barnfire and PDT were accurately propagating uncertainties for FEDS. While, the two criticality

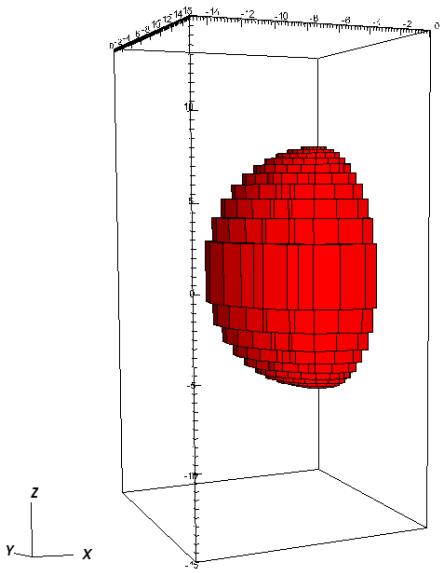

Fig. 8. A 32-sided polygon in the X-Y plane, extruded into 19 extrusion steps along the Z axis was constructed in order to approximate Godiva.

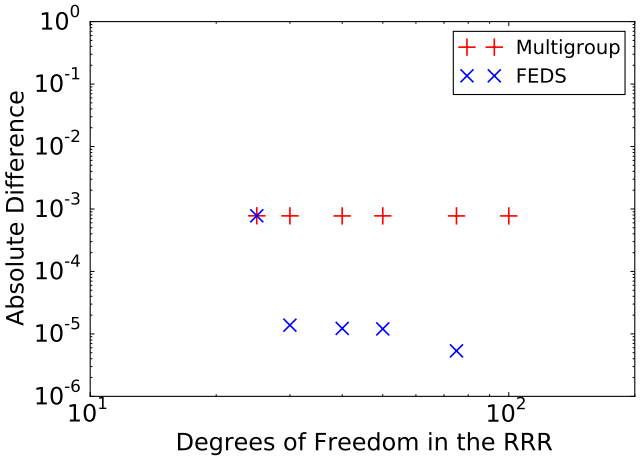

Fig. 9. This plot shows the discrepancy between the multigroup and FEDS values for k_{eff} from a reference solution which is fully-resolved in energy for validation problem 2 (the reference solution in this case is the FEDS value for k_{eff} with 100 elements in the RRR).

benchmarks demonstrated that FEDS converged much faster than multigroup for the energy resolution in the RRR.

In the future, PDT will be capable of doing 1-D spherical-geometry discrete-ordinates solves, and we will reattempt Validation Problem 2 using the spherical mesh with increased levels of angular and spatial refinement. In addition, we plan to split up the fission source term in the neutron transport equation into prompt and delayed terms and generate multigroup and FEDS cross sections for these terms separately. For the prompt fission term we plan to use a double-differential fission matrix, and for delayed neutrons we plan to use a different

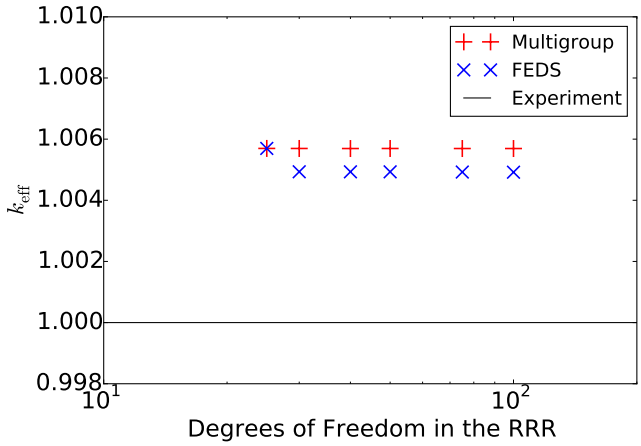

Fig. 10. This plot demonstrates how far the multigroup and FEDS values for k_{eff} are from the experimental value for Godiva. This discrepancy is mostly due to spatial and angular discretization error.

fission spectrum for each delayed neutron precursor flavor. This will provide better estimates for k_{eff}, and pave the way to using FEDS for time-dependent simulations later on.

V. ACKNOWLEDGMENTS

We would like to thank Teresa Bailey, Peter Brown, Robert Cavallo, Andrew Till, and Donald Bruss for openly discussing any challenges we encountered during this project.

REFERENCES

1. A. T. TILL, *Finite Elements with Discontiguous Support for Energy Discretization in Particle Transport*, Ph.D. thesis, Texas A&M University (2015).
2. D. E. BRUSS, *Adjoint-Based Uncertainty Quantification for Neutron Transport Calculations*, Ph.D. thesis, Texas A&M University (2016).
3. D. MUIR, R. BOICOURT, and A. KAHLER, "The NJOY Nuclear Data Processing System, Version 2012," Tech. rep., LA-UR-12-27079 (2012).
4. A. N. M. MATHIS, MARK M. and M. L. ADAMS, "A General Performance Model for Parallel Sweeps on Orthogonal Grids for Particle Transport Calculations," Tech. rep., Department of Computer Science, Texas A&M University (2000).
5. J. T. GOORLEY, M. R. JAMES, T. E. BOOTH, F. BROWN, J. BULL, L. J. COX, J. DURKEE, J. ELSON, M. FENSIN, R. FORSTER, ET AL., "Initial MCNP6 release overview-MCNP6 version 1.0," Tech. rep.